small methods

Supporting Information

for *Small Methods,* DOI: 10.1002/smtd.202200142

An Anti-Biofouling Flexible Fiber Biofuel Cell Working in the Brain

Yue Guo, Chuanrui Chen, Jianyou Feng, Liyuan Wang, Jiajia Wang, Chengqiang Tang, Xuemei Sun, and Huisheng Peng**

Supporting Information

Experimental Section

Chemicals and reagents. Glucose oxidase (GOx), dopamine hydrochloride and 5% Nafion solution were purchased from Sigma Aldrich Co., Ltd. Glucose was purchased from TCI (Shanghai) Development Co., Ltd. Glutaraldehyde was purchased from Sinopharm Chemical Reagent Co., Ltd. Platinum on carbon (Pt/C) was purchased from Johnson Matthey. Tetrathiafulvalene (TTF), bovine serum albumin (BSA) and 2-methacryloyloxyethyl phosphorylcholine (MPC) were purchased from Bide Pharmatech Ltd. Fluorescein-tagged bovine serum albumin (FITC-BSA) was purchased from Bioss Inc. Tris-hydrochloride (Tris-HCl) buffer solution was purchased from Nanjing SenBeiJia Biological Technology Co., Ltd. Phosphate buffered saline (PBS, 0.1 M, pH=7.4) was purchased from Solarbio Science and Technology Co., Ltd.

Fabrication of flexible fiber biofuel cell (BFC). CNT fibers were synthesized by floating catalyst chemical vapor deposition in a tube furnace with the reaction temperature of 1200 °C, with thiophene and ferrocene as catalysts, flowing ethanol as carbon source, argon (200 sccm) as carrier gas, and hydrogen (1600 sccm) as reducing gas. For bioanode preparation, the CNT fiber electrode was firstly immersed in 20 mM TTF ethanol/acetone (9:1, v/v) solution overnight and then washed with deionized water. Then, it was immersed overnight at 4℃ in 10-80 $mg \cdot mL^{-1}$ GOx in 0.1 M PBS containing 0.15% glutaraldehyde. For cathode preparation, the Pt/C catalyst dispersion was firstly prepared by mixing Pt/C (10 mg) with mixture of deionized water (750 μL), ethanol (220 μL) and 5% Nafion solution (30 μL), followed by sonication for 1 h to obtain homogeneous solution. The CNT fiber electrode was coated with the Pt/C catalyst dispersion, and then left dried in air.

Modification of polydopamine-2-methacryloyloxyethyl phosphorylcholine (PDA-MPC) layer on flexible fiber BFC. The fabricated CNT fiber bioanode and cathode were immersed in 2 $mg \cdot mL^{-1}$ dopamine Tris-HCl buffer solution (10 mM, pH=8.8) at room temperature for 1 h, thus the electrode surfaces can be coated with PDA layers by oxidative self-polymerization of dopamine. The electrodes were then washed thoroughly with deionized water. Next, the bioanode and cathode were immersed in 5

mg·mL^{-1} MPC Tris-HCl buffer solution (10 mM, pH=8.8) for 12 h, and then rinsed with deionized water.

Implementation of the strain sensor. The preparation of the strain sensor was described previously.[1] The whole self-powered sensing system was constructed *in vitro*, with the fiber BFC situated in the glucose solution as the power source. During the test, the strain sensor was stretched by the universal testing instrument, and the partial voltage of the sensor was recorded.

Apparatus and measurements. Scanning Electron Microscopy (SEM, Zeiss Ultra 55) was used to characterize the morphology of fiber electrodes. X-ray photoelectron spectroscopy (XPS) was recorded on Thermo Scientific K-Alpha. Atomic force microscopy (AFM, Bruker Dimension Icon) was used to analyze the thickness of PDA-MPC modification layer. Electrochemical measurements were performed on Metrohm Autolab M204 controlled by NOVA software (version 2.1.3) and CHI660e electrochemical workstation. To characterize the electrochemical properties of fiber bioanode or cathode, the three-electrode system was used. The working electrode was the fabricated fiber bioanode or cathode, the counter electrode was platinum wire, and the reference electrode was Ag/AgCl (3 M KCl) electrode, respectively. To characterize the power output of the fiber BFC, a two-electrode system was used, with the bioanode as the counter and reference electrode and the cathode as the working electrode. The calculation of the power density of the fiber BFC was based on the geometrical area of the fiber electrodes. The force–compression curves of CNT fiber, gold wire and carbon fiber were tested using universal testing instrument (Hengyi). The diameter of gold wire and carbon fiber was 50 μm and 7 μm, respectively. The fiber materials were compressed with a velocity of 0.6 mm/min. Static water contact angles were evaluated by using a contact angle goniometer in order to explore the hydrophilicity of PDA-MPC modified, PDA modified and unmodified CNT fiber electrodes. To evaluate the protein adsorption, PDA-MPC modified, PDA modified and unmodified CNT fiber electrodes were incubated with 1 mg·mL^{-1} FITC-BSA for 2 h. Then the electrodes were washed with deionized water thoroughly followed by confocal fluorescence microscopic imaging performed on scanning laser confocal microscope (Nikon C2+). The photoacoustic images were collected and analyzed using a Vevo LAZR Imaging System (Fuji Film VisualSonics Inc).

In vivo experiments. All the animal experiment procedures were approved by Animal Experimentation Committee of Fudan University. All experimental animals were treated in accordance with the guidelines for the care and use of experimental animals described by the National Institutes of Health and Fudan University. Female mice (ICR, 4-6 weeks old) were purchased from Shanghai Jiesijie experimental animal Co., Ltd and kept on a 12:12 h light-dark schedule with food and water *ad libitum*. The mouse was anesthetized with 4% isoflurane for 3-5 min. Then, it was put onto a stereotaxic frame and maintained with 1.5% isoflurane under the inhalational condition. The craniotomy was made over the mouse cortex and the dura was incised and resected. Then the flexible fiber BFC was implanted into the cortex through tungsten wire-assisted strategy. After the electric circuit was connected, the power output performance of BFC was recorded *in vivo*.

Immunohistochemistry test. Mice were sacrificed after being implanted with the fiber BFC for one week and one month. The removed brains from mice were fixed with 4% paraformaldehyde overnight and then sliced to 4 μm-thick cross-sectional sections. For the immunofluorescence staining, the brain slices should be firstly placed in a microwave oven for antigen retrieval in citrate buffer (0.01 M, pH 6.0). Mouse anti-neuronal nuclear antigen (NeuN, 1:8000, GB13138, Servicebio), rabbit anti-glial fibrillary acidic protein (GFAP, 1:500, GB11096, Servicebio) and rabbit anti-ionized calcium-binding adapter molecule-1 (Iba-1, 1:500, GB13105, Servicebio) were used as primary antibody. Alexa Fluor® 488-labelled Goat Anti-Mouse IgG (H+L) (1:500, GB23303, Servicebio) and Cy3 conjugated Goat Anti-Rabbit IgG (H+L) (1:300, GB21303, Servicebio) were used as secondary antibody. All the cell nuclei were labelled by 4′,6-diamidino-2-phenylindole (DAPI) Fluoromount-G® (0100-20, Southern Biotech). The immunofluorescence stained brain slices were observed under fluorescence microscopy (Olympus BX51).

Statistical analysis. Statistical Product and Service Solutions (SPSS) software was used to assess the statistical significance of the comparison studies in this work. Normality of data distribution was tested via Shapiro–Wilk test. For the anti-biofouling performance characterization, paired two-sided Student's t-tests were used, and significance threshold was placed at $*p < 0.05$. Three technical repeats were performed in all experiments and error bars represent standard deviations.

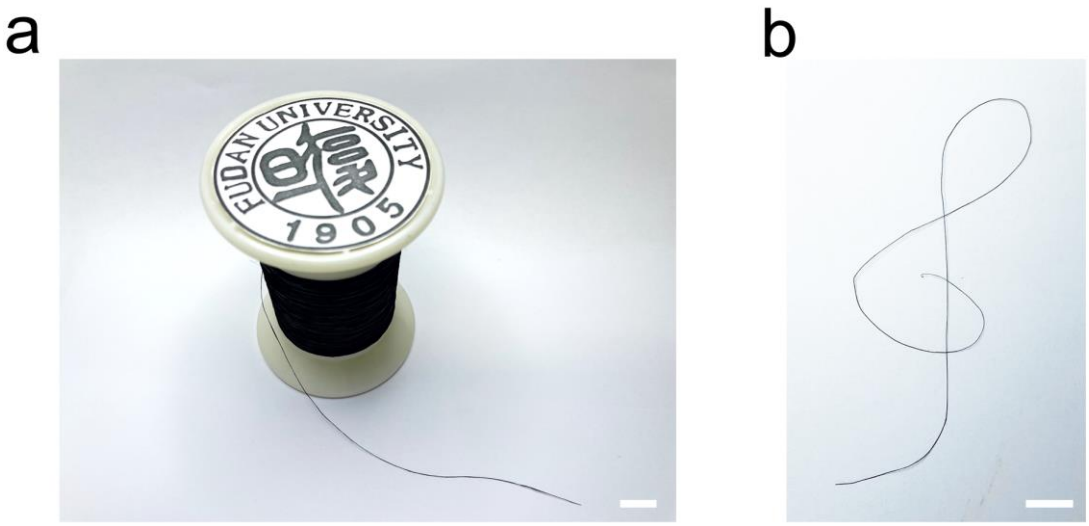

Figure S1. a) Photograph of a roll of CNT fiber. **b**) Photograph of a CNT fiber in the shape of treble clef. Scale bar, **a**) 1 cm; **b**) 0.5 cm.

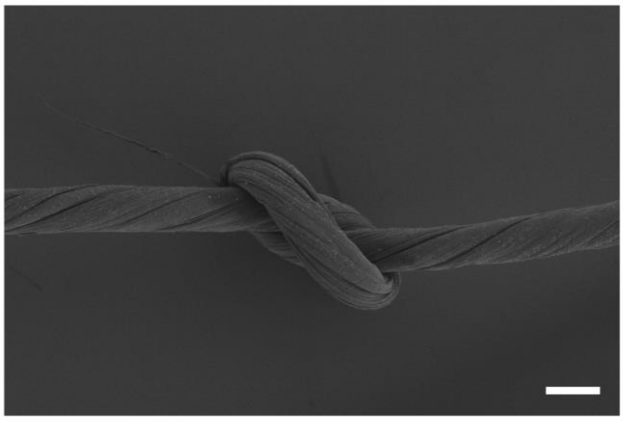

Figure S2. SEM image of a knotted CNT fiber electrode showing high flexibility. Scale bar, 100 μm.

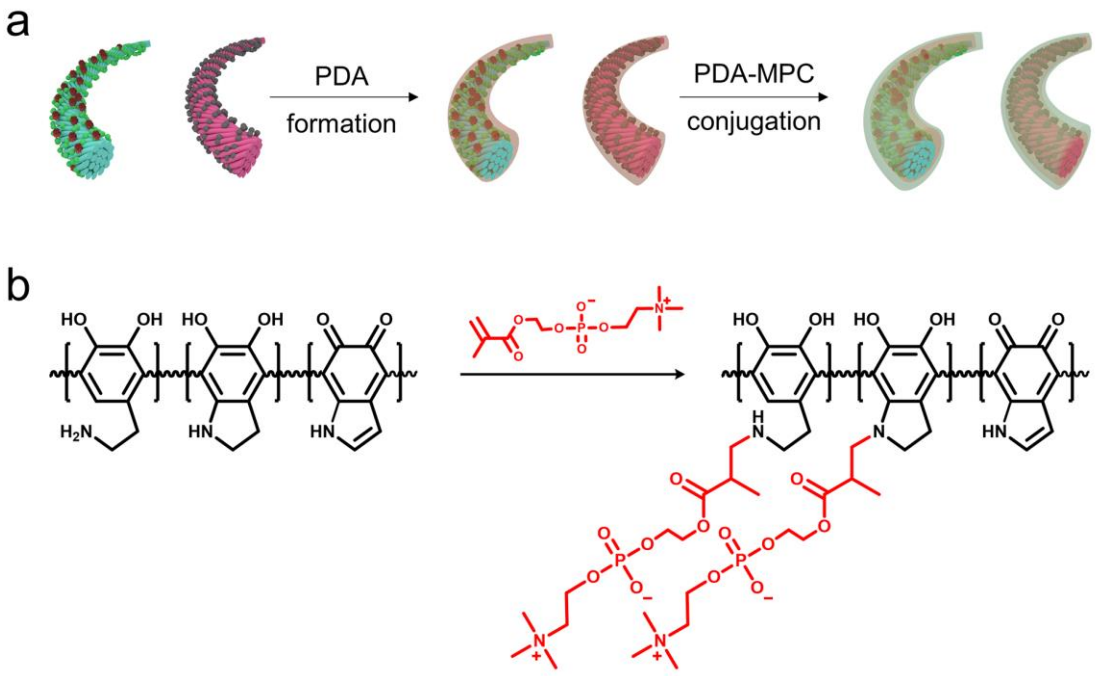

Figure S3. a) The schematic diagram of modification procedure of PDA-MPC layer on fiber electrodes. **b**) The chemical reaction between PDA and MPC.

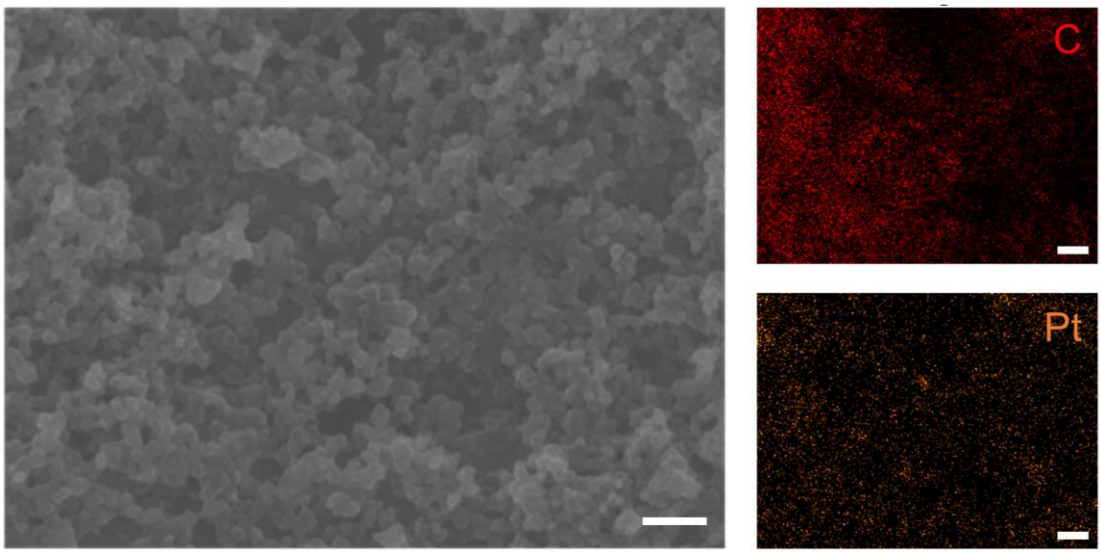

Figure S4. The elemental (C and Pt) mapping images of fiber cathode. Scale bar, 500 nm.

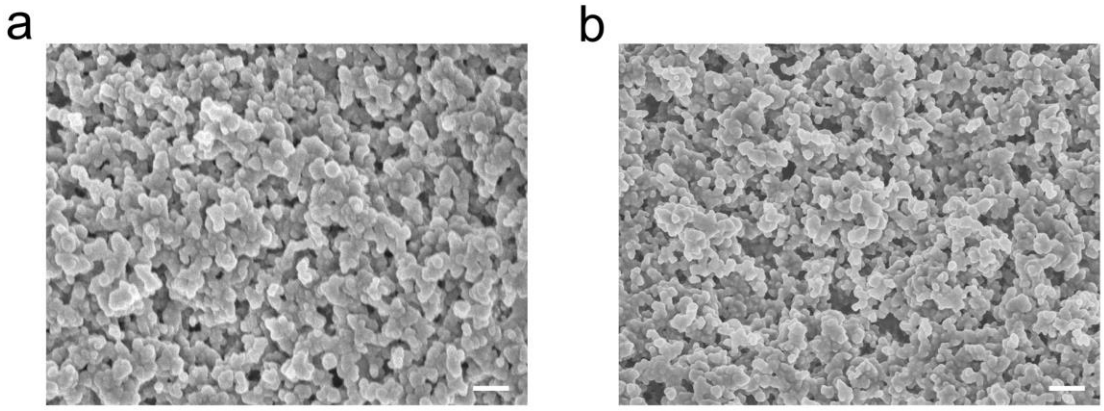

Figure S5. SEM images of **a**) PDA-MPC modified and **b**) unmodified fiber cathodes. Scale bar, 400 nm.

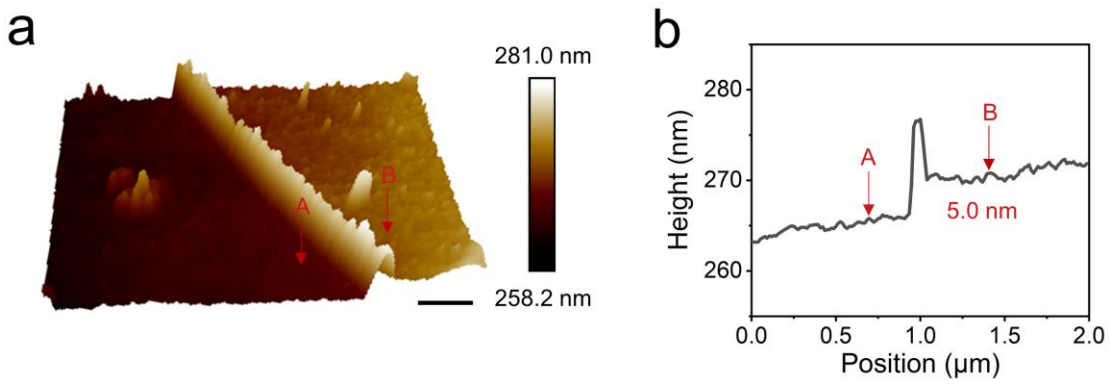

Figure S6. a) AFM image of PDA-MPC layer on silicon substrate. Scale bar, 0.5 μm. **b**) The thickness of PDA-MPC layer.

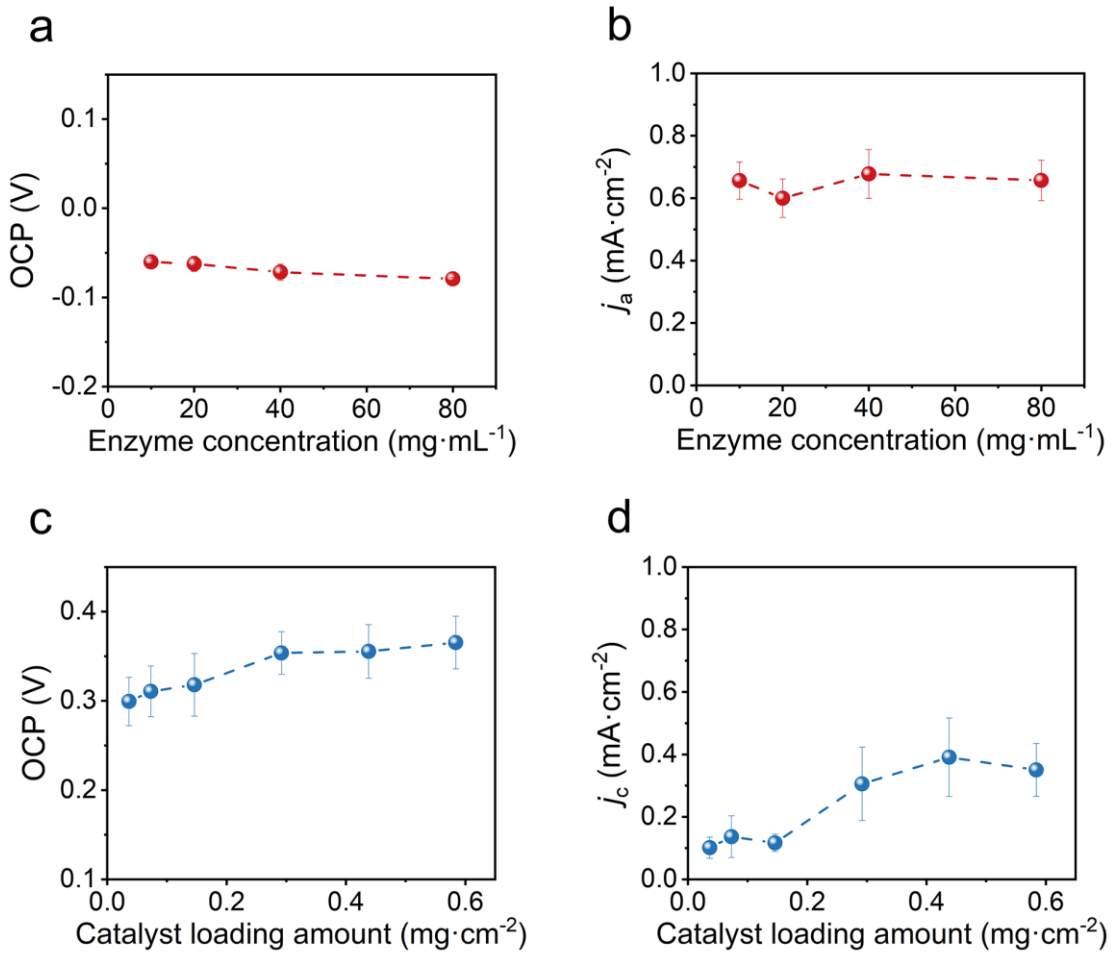

Figure S7. Evolution of **a**) open-circuit potential and **b**) anodic current density (at 0.15 V) of fiber bioanode modified with different concentrations of enzyme solution in 6 mM glucose. Evolution of **c**) open-circuit potential and **d**) cathodic current density (at 0.15 V) of fiber cathode with different catalyst loading amounts in air-saturated PBS. Error bars: standard deviations; n = 3.

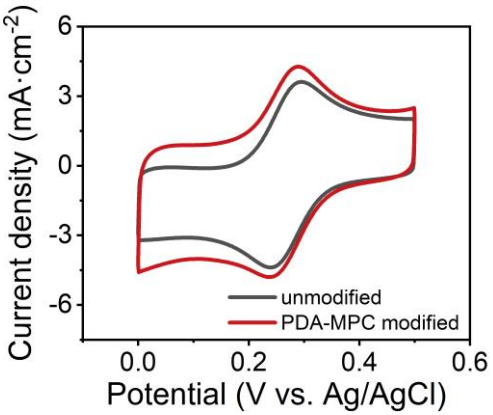

Figure S8. Cyclic voltammograms of PDA-MPC modified and unmodified CNT electrodes in PBS containing 5 mM potassium ferricyanide.

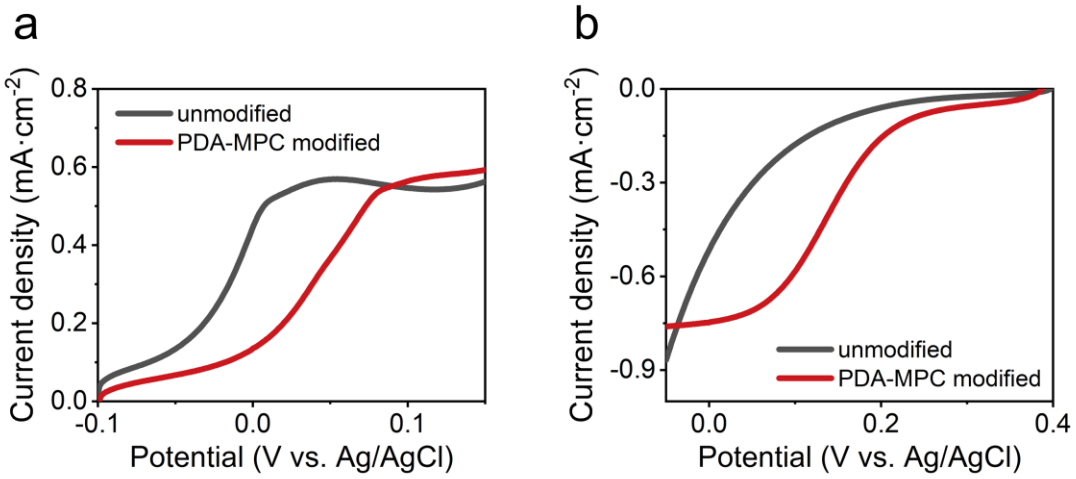

Figure S9. a) Linear sweep voltammograms (LSVs) of PDA-MPC modified and unmodified fiber bioanodes in 6 mM glucose. **b**) LSVs of PDA-MPC modified and unmodified fiber cathodes in air-saturated PBS.

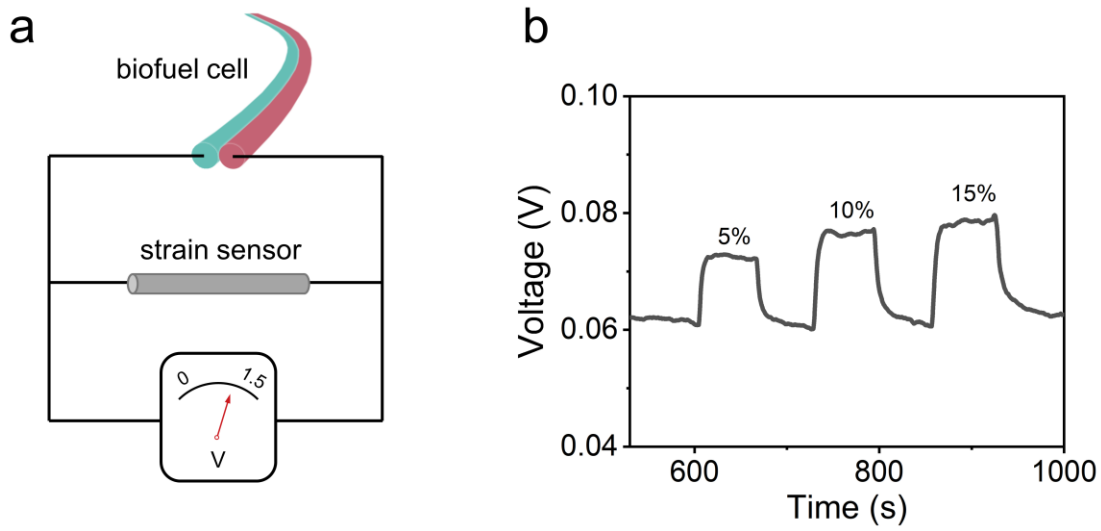

Figure S10. a) The schematic diagram of fiber BFC powering a strain sensor *in vitro*. The biofuel cell was situated in the glucose solution. **b**) Response of the sensor to the change of strain.

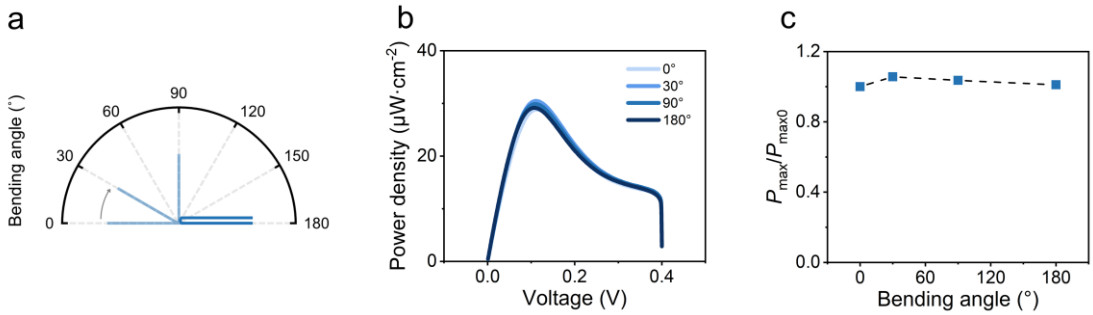

Figure S11. a) The schematic diagram of fiber BFC bending at different angles. The length of fiber BFC was 1 cm. **b**) The power density–voltage curves of fiber BFC bending at different angles. **c**) The calculated relative change of maximal power density of fiber BFC bending at different angles.

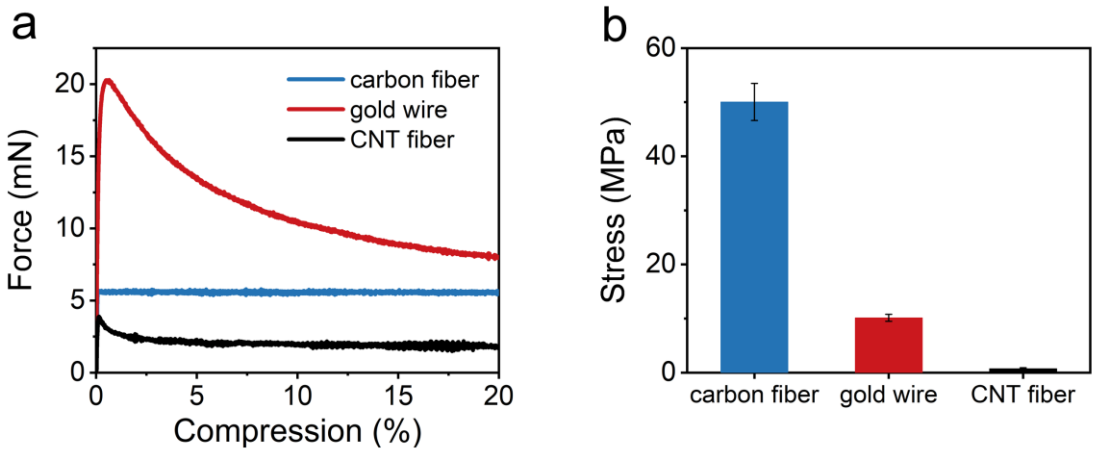

Figure S12. a) The force–compression curves of CNT fiber, carbon fiber and gold wire. **b**) The internal stress of the CNT fiber, carbon fiber and gold wire under compression. Error bars: standard deviations; n = 3.

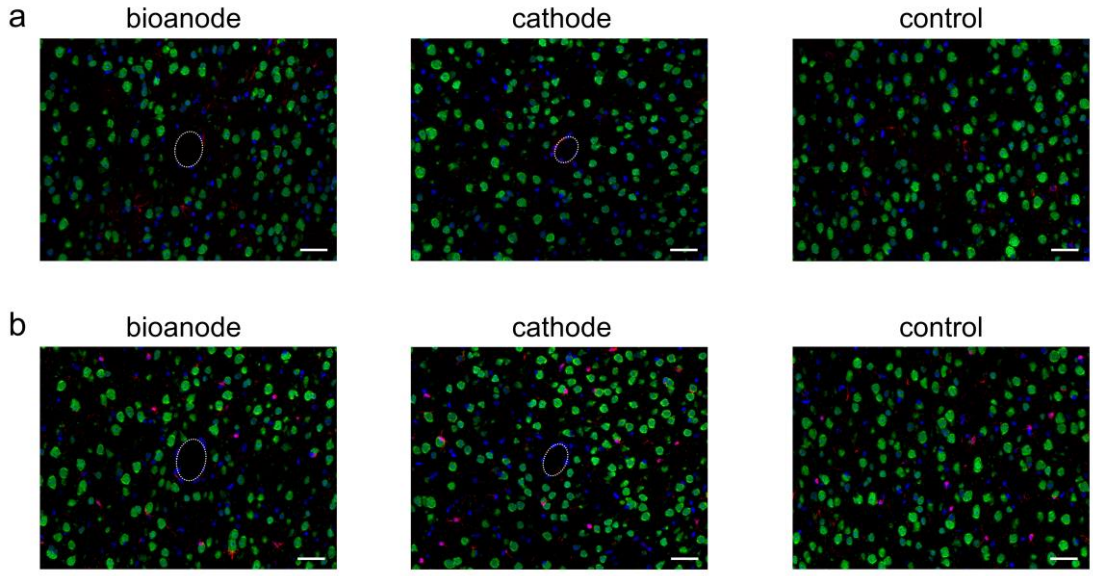

Figure S13. Immunohistochemical staining images of cross-sectional brain slices at 1 week after implantation of fiber BFC. Blue, red and green colors correspond to DAPI (label of cell nuclei), **a**) GFAP (label of astrocytes) or **b**) Iba-1 (label of microglia), and NeuN (label of neuron somata), respectively. The white dotted circles indicate the position of fiber bioanode or cathode. Scale bar, 50 μm.

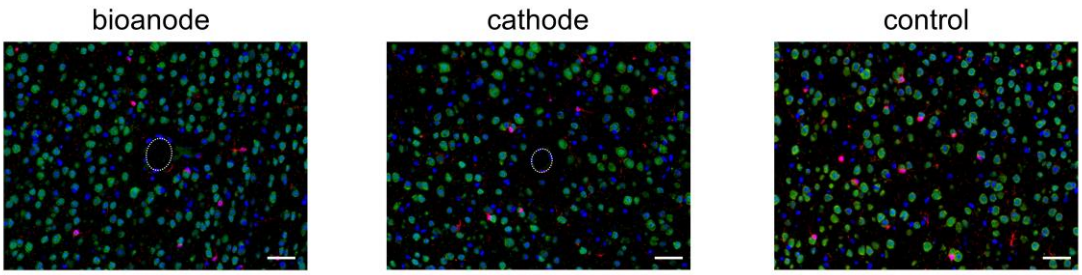

Figure S14. Immunohistochemical staining images of cross-sectional brain slices at 1 month after implantation of fiber BFC. Blue, red and green colors correspond to DAPI (label of cell nuclei), Iba-1 (label of microglia) and NeuN (label of neuron somata), respectively. The white dotted circles indicate the position of fiber bioanode or cathode. Scale bar, 50 μm.

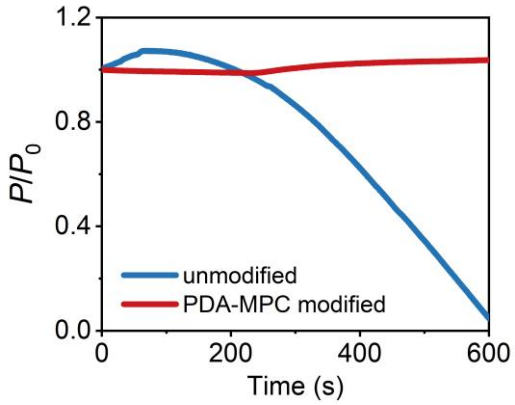

Figure S15. The power output change at 0.2 μA·cm^{-2} of PDA-MPC modified and unmodified BFCs after implantation for 2 h.

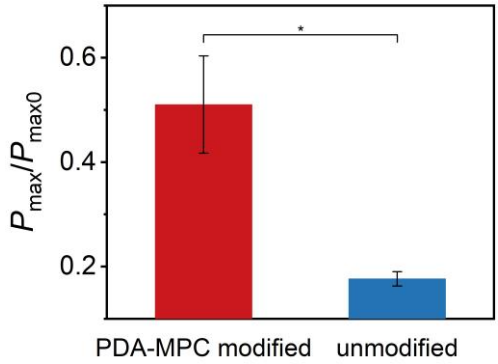

Figure S16. The relative maximal power output of PDA-MPC modified and unmodified BFC after implanted into the mouse brain for 1 h. The values represent means ± standard deviations (n = 3; *p < 0.05, paired two-sided Student's t-test).

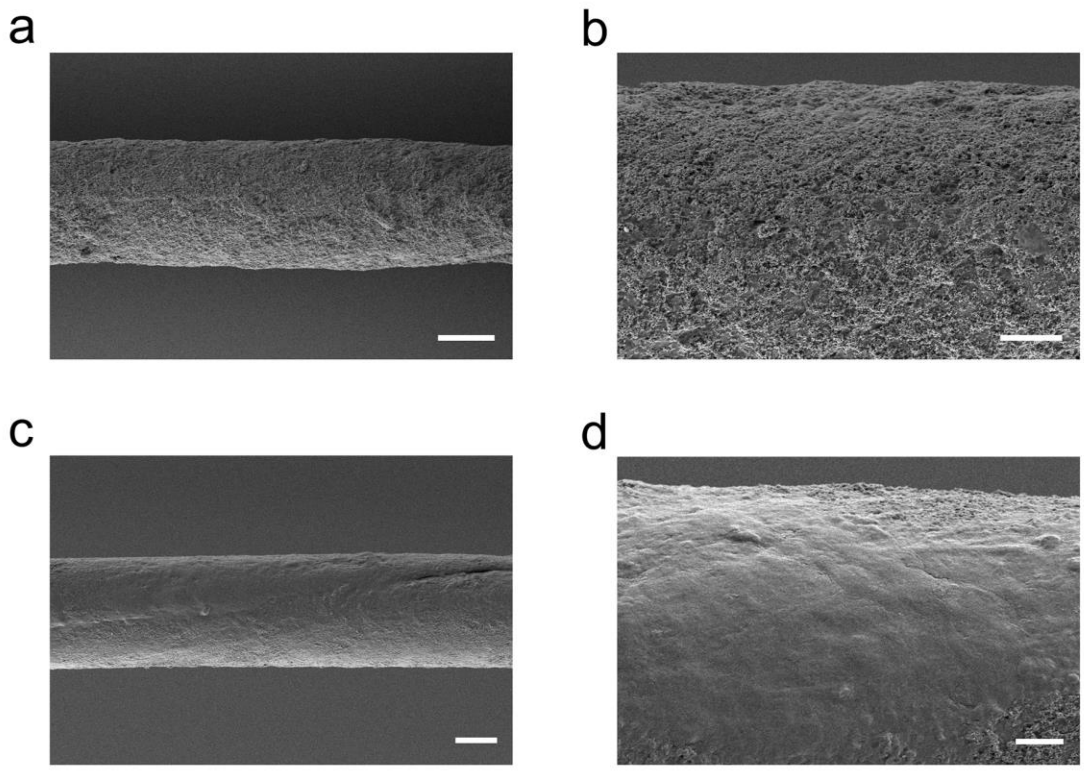

Figure S17. SEM images of **a, b**) PDA-MPC modified and **c**, **d**) unmodified fiber cathodes after implanted into the mouse brain for 1 h. Scale bar, **a, c**) 30 μm; **b, d**) 10 μm.

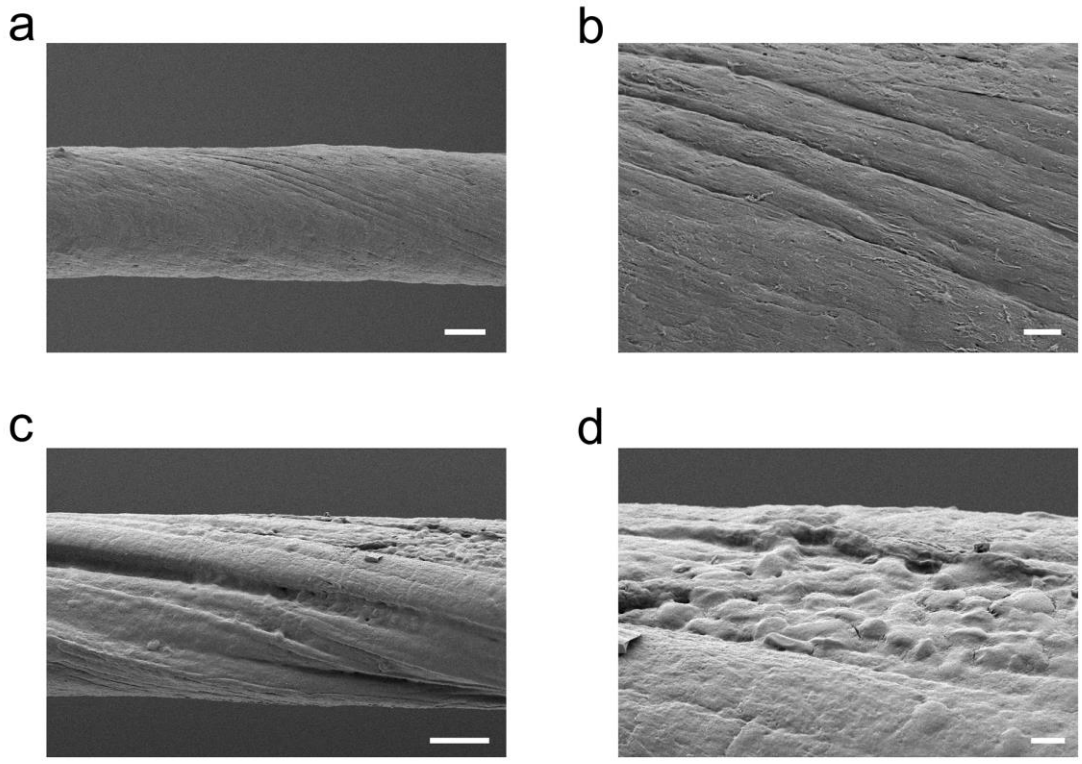

Figure S18. SEM images of **a**, **b**) PDA-MPC modified and **c**, **d**) unmodified fiber bioanodes after implanted into the mouse brain for 1 h. Scale bar, **a, c**) 30 μm; **b, d**) 5 μm.

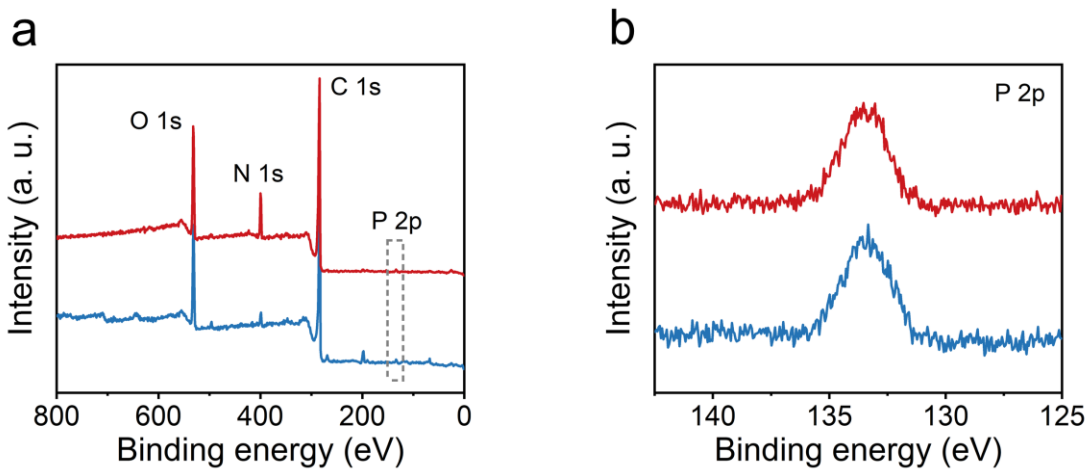

Figure S19. a) XPS spectra of PDA-MPC modified electrode before (blue curve) and after implantation (red curve). **b**) High-resolution XPS spectra of P 2p peak of PDA-MPC modified electrode before (blue curve) and after implantation (red curve).

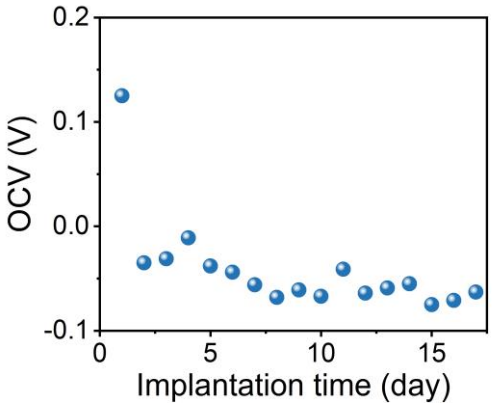

Figure S20. The open-circuit voltage of an unmodified BFC *in vivo*.

Table S1. Comparison of areal power density and operational lifetime of our work with previous reported fiber-based BFC implanted in mammals.

Animal	Implant position	Anode	Cathode	Anti-biofouling modification	Power density *in vitro*	Power density *in vivo*	Operational lifetime	Ref.
Mouse	Brain	CNT fiber/TTF/GOx	CNT fiber/PtC	PDA-MPC	32.6 μW·cm^{-2}	2.5-4.4 μW·cm^{-2}	> 1 month	This work
Rat	Brain	Gold wire/AuNPs/CDH	Gold wire/AuNPs/BOx	-	7 μW·cm^{-2}	2 μW·cm^{-2}	Several hours	[2]
Mouse	Jugular vein	Carbon fiber/NR/GOx-BSA	Carbon fiber/PAMAM-PtNP	-	200 μW·cm^{-2}	95 μW·cm^{-2}	24 h	[3]
Rabbit	Ear vein	Gold wire/PLL-VK_3/Dp/PLL-NAD^+/GDH	Carbon paper/KB/BOx/KB	MPC polymer	N/A	0.42 μW	N/A	[4]
Mouse	Abdominal cavity	Carbon fiber/CNT/PVI-[$Os(bpy)_2Cl$]/GOx/ PVI-[$Os(bpy)_2Cl$]	Carbon fiber/PTFE-CNT/CNT/BOx/PTFE-CNT	-	20.4 μW	8.5 μW	N/A	[5]
Mo	Hear	Carbon	Carbon	MPC	N/	16.	N/A	[5

use	t	fiber/CNT/PVI-[Os(bpy)$_2$Cl]/GOx/ PVI-[Os(bpy)$_2$Cl]	fiber/PTFE-CNT/ CNT/BOx/PTFE-CNT	polymer	A	3 μW]

AuNP: gold nanoparticle; CDH: cellobiose dehydrogenase; BOx: bilirubin oxidase; NR: neutral red; PAMAM: polyamidoamine dendrimer; PtNP: platinum nanoparticle; PLL: poly-L-Lysine; VK_3: vitamin K_3; Dp: diaphorase; NAD^+: nicotinamide adenine dinucleotide; GDH: glucose dehydrogenase; PVI-[Os(bpy)$_2$Cl]: polyvinylimidazole-[Os(bipyridine)$_2$Cl]; PTFE: poly(tetrafluoroethylene)

Table S2. Comparison of volume power density and operational lifetime of our work with previous reported BFC based on bulky structure implanted in mammals.

Animal	Implant position	Anode	Cathode	Anti-biofouling modification	Power density *in vivo*	Operational lifetime	Ref.
Mouse	Brain	CNT fiber/TTF/GOx	CNT fiber/PtC	PDA-MPC	1.3-2.3 mW·cm^{-3}	**>** 1 month	This work
Rat	Abdominal cavity	Graphite disc/GOx, catalase, ubiquinone	Graphite disc/PPO, quinhydrone	Dialysis bag, exPTFE membrane	24.4 μW·cm^{-3}	11 days	[6]
Rat	Abdominal cavity	CNT pellet/GOx	CNT pellet/laccase	Dialysis bag, silicone tube, Dacron sleeve	161 μW·cm^{-3}	9 days	[7]
Rabbit	Abdominal cavity	CNT pellet/GOx, catalase, naphtoquinone	CNT pellet/laccase, chitosan-genipin	Chitosan, Dacron lattice	16 μW·cm^{-3}	2 months	[8]

PPO: polyphenol oxidase; exPTFE: expanded poly(tetrafluoroethylene)

References

[1] L. Lu, Y. Zhou, J. Pan, T. Chen, Y. Hu, G. Zheng, K. Dai, C. Liu, C. Shen, X. Sun, H. Peng, *ACS Appl. Mater. Interfaces* **2019**, *11*, 4345.

[2] V. Andoralov, M. Falk, D. B. Suyatin, M. Granmo, J. Sotres, R. Ludwig, V. O. Popov, J. Schouenborg, Z. Blum, S. Shleev, *Sci. Rep.* **2013**, *3*, 3270.

[3] F. C. P. F. Sales, R. M. Iost, M. V. A. Martins, M. C. Almeida, F. N. Crespilho, *Lab Chip* **2013**, *13*, 468.

[4] T. Miyake, K. Haneda, N. Nagai, Y. Yatagawa, H. Onami, S. Yoshino, T. Abe, M. Nishizawa, *Energ. Environ. Sci.* **2011**, *4*, 5008.

[5] S. Yin, X. Liu, Y. Kobayashi, Y. Nishina, R. Nakagawa, K. Kimura, T. Miyake, *Biosens. Bioelectron.* **2020**, *165*, 112287.

[6] P. Cinquin, C. Gondran, F. Giroud, S. Mazabrard, A. Pellissier, F. Boucher, J. P. Alcaraz, K. Gorgy, F. Lenouvel, S. Mathe, P. Porcu, S. Cosnier, *Plos One* **2010**, *5*, e10476.

[7] A. Zebda, S. Cosnier, J. P. Alcaraz, M. Holzinger, A. Le Goff, C. Gondran, F. Boucher, F. Giroud, K. Gorgy, H. Lamraoui, P. Cinquin, *Sci. Rep.* **2013**, *3*, 1516.

[8] S. El Ichi-Ribault, J. P. Alcaraz, F. Boucher, B. Boutaud, R. Dalmolin, J. Boutonnat, P. Cinquin, A. Zebda, D. K. Martin, *Electrochim. Acta* **2018**, *269*, 360.